

# Dynamic Light Scattering and Pulsed Gradient Spin-Echo NMR Measurements of Diffusion in Polystyrene-Poly(vinyl methyl ether)-Toluene Solutions

P. J. Daivis,\*† D. N. Pinder, and P. T. Callaghan

Department of Physics and Biophysics, Massey University, Palmerston North, New Zealand

Received December 4, 1990; Revised Manuscript Received July 22, 1991

**ABSTRACT:** The results of dynamic light scattering (DLS) and pulsed gradient spin-echo (PGSE) NMR measurements on ternary solutions of poly(vinyl methyl ether) (PVME) and polystyrene (PS) in toluene are presented. Samples with four different values (0.001, 0.056, 0.114, and 0.246) of  $x$ , the ratio of PS concentration to the total polymer concentration, were studied. The total polymer concentration  $C$  was varied between approximately 70 and 500 kg m<sup>-3</sup> for each value of  $x$ . The molar masses of the PVME and PS were 110 000 g mol<sup>-1</sup>, and the measurement temperature was  $T = 30^\circ\text{C}$ . DLS experiments were performed on the samples with  $x = 0.056, 0.114$ , and  $0.246$ . The DLS experiments on these samples gave a single mode of decay from which a diffusion coefficient was extracted. PGSE experiments were performed on all of the samples. The PS self-diffusion coefficient was obtained from PGSE experiments on the  $x = 0.056, 0.114$ , and  $0.246$  sets of samples, and the self-diffusion coefficient of the PVME was obtained from measurements on the  $x = 0.001$  samples. The diffusion coefficients obtained from the DLS experiments were found to be equal within experimental errors to the PS self-diffusion coefficients obtained from PGSE NMR experiments on the same samples. The DLS diffusion coefficient did not vary measurably with  $x$  at a given value of  $C$  for the molar masses and concentrations studied here.

## 1. Introduction

A dynamic light scattering (DLS) experiment on a semidilute ternary polymer solution composed of two polymers and a solvent that is good for both polymers is, in general, expected to yield a correlation function consisting of a sum of two exponential decays, with the fast mode describing a cooperative diffusion process and the slow mode describing an exchange or interdiffusion process. Under certain experimental conditions, the amplitude of the fast mode can be made negligibly small and the decay rate of the slower mode becomes proportional to the self-diffusion coefficient of one of the polymer components of the solution. This is true for the polystyrene-poly(vinyl methyl ether)-toluene system where the PVME and toluene are isorefractive, the polystyrene is present only at trace concentrations, the polymers are mutually compatible, and the solvent is good for both of them. Several groups have used DLS to measure the self-diffusion coefficient of a trace of polystyrene in PVME-toluene or similar solutions,<sup>1-12</sup> and a recent study of the PS-PVME-(*o*-fluorotoluene) system by Chang et al.<sup>10</sup> using forced Rayleigh scattering has experimentally confirmed, within a limited total polymer concentration range, that  $D_s$  is in fact measured by DLS under these conditions.

Few experimental studies have investigated the range of experimental conditions over which the amplitude of the fast mode remains negligible and the diffusion coefficient of the slow mode  $D_I$  is equal to  $D_s$ . Parameters which would need to be varied independently in such studies are the compatibility of the polymers, the solvent quality, the relative concentrations of the polymers, the total polymer concentration, the polymer molar masses, and the optical contrast of the two polymers with the solvent. The results of preliminary experiments on the PS-PVME-carbon tetrachloride system<sup>13</sup> suggest that near the cloud point,  $D_I \neq D_s$ , in agreement with the theoretical predictions of Benmouna et al.<sup>14</sup>

In this work, the effects of changes in  $x$ , the ratio of PS concentration to the total polymer concentration, and  $C$ , the total polymer concentration, on the results of DLS experiments on PS-PVME-toluene solutions are investigated. The results are directly compared with the values of  $D_s$  obtained from pulsed gradient spin-echo (PGSE) NMR measurements.

## 2. Theory

**Dynamic Light Scattering.** The theory of dynamic scattering from ternary polymer solutions has been discussed elsewhere.<sup>14,15</sup> Here, it is sufficient to recall some results for a special case discussed by Benmouna et al.<sup>14</sup>

Benmouna et al. found two relaxation modes in the dynamic structure factor  $S(\mathbf{q}, \tau)$  for scattering from semidilute polymer-polymer-solvent systems. They identified the faster mode as a cooperative mode and the slower one as an interdiffusion mode. The theory of Foley and Cohen<sup>15</sup> gives similar results to those of Benmouna et al. but does not contain explicit expressions for the diffusion coefficients.

One of the special cases considered by Benmouna et al. is particularly relevant to this work: that of two interacting polymers with equal molar masses and sizes, one having no contrast with the solvent, in a solvent of the same solvent quality for both polymers.

In this case, the two decay rates are given by

$$\Gamma_I = q^2 D_I(q) = \Gamma_S(q) [1 - 4A_2 MCx(1-x)P(q)\chi/v] \quad (1)$$

and

$$\Gamma_C = q^2 D_c(q) = \Gamma_S(q) [1 + 2A_2 MCP(q)] \quad (2)$$

where  $q$  is the magnitude of the scattering vector,  $x = C_1/C$  is the relative concentration of the visible polymer,  $C = C_1 + C_2$  is the total polymer concentration,  $A_2$  is a generalized virial coefficient which may depend on  $C$  (expressing the dependence of the osmotic pressure on the total polymer concentration),  $v$  is the excluded-volume parameter (assumed to be the same for both polymers), and  $\chi$  ( $=\chi_{12}$ ) is the Flory interaction parameter for

\* Author to whom all correspondence should be addressed.

† Present address: Research School of Chemistry, The Australian National University, GPO Box 4, Canberra, ACT 2601 Australia.

polymer-polymer interactions.<sup>14,16,17</sup>  $\Gamma_S(q)$  is the "bare" decay rate, i.e., the decay rate of the self-dynamic structure factor<sup>17</sup> which in this theory is given by

$$\Gamma_S = q^2 \frac{k_B T}{N \zeta P(q)} = \frac{q^2 D_s}{P(q)} \quad (3)$$

where  $N$  is the degree of polymerization and  $\zeta$  is the monomeric friction factor. If the form factor  $P(q)$  is equal to 1, as it is expected to be at low molar masses, a  $q$ -independent effective diffusion coefficient is obtained. Since the Rouse form of the friction factor,  $N\zeta$ , appears in eq 3, it is clear that this theory does not account for the effect of hydrodynamic interactions or entanglements on chain dynamics.

The mode amplitudes  $A_C$  and  $A_I$  determine whether both or only one of the modes are actually observed. Expressions for the mode amplitudes are given by Benmouna et al.<sup>14</sup> and Borsali et al.<sup>17</sup> For the special case considered here, the following results are found. In the limit of low values of  $x$ , the amplitude of the cooperative mode approaches zero, so that only the interdiffusion mode is measured. At intermediate values of  $x$ , both modes are expected to contribute to  $S(q, \tau)$ , even though one of the polymers is "invisible". In the limit as  $x$  approaches 1, the amplitude of the interdiffusion mode goes to zero and the cooperative mode dominates. (Note that these considerations apply to solutions of interacting polymers, not infinitely dilute solutions.)

Equations 1 and 3 show that when  $P(q) = 1$  and  $x \rightarrow 0$ ,  $\Gamma_I = q^2 D_s$ . This is the condition which has been invoked in measurements of  $D_s$  in "optical tracer" dynamic light scattering experiments. However, eq 1 indicates that the degree to which  $D_I$  approximates  $D_s$  depends not only upon the value of  $x$  but also upon the thermodynamic quantities  $A_2$  and  $\chi/v$ . When  $\chi/v$  tends to zero,  $\Gamma_I$  becomes equal to  $\Gamma_S(q)$  regardless of the value of  $x$ . Such a situation is realized when the polymers are compatible and the solvent is good for both of them. On the other hand, if  $\chi/v$  becomes large,  $D_I$  may remain different from  $D_s$  even at very low values of  $x$ . In the case of PS-PVME blends, it is known that  $\chi$  is small and negative<sup>18,19</sup> and that toluene is a good solvent for PS and probably also for PVME. Therefore, we expect that  $D_I = D_s$ , regardless of the value of  $x$ .

**Pulsed Gradient Spin-Echo NMR.** The theory of pulsed gradient spin-echo NMR has been reviewed before.<sup>20</sup> Only a brief recapitulation of relevant points will be given here.

The result of Stejskal and Tanner's analysis<sup>21</sup> of the PGSE experiment is the standard equation for the spin-echo amplitude  $A$

$$A(2\tau, G) = A_0 \exp(-2\tau/T_2) \exp[-D_s \gamma^2 G^2 \delta^2 (\Delta - \delta/3)] \quad (4)$$

where  $G$  is the magnitude of the applied magnetic field gradient,  $\tau$  is the time between the  $\pi$  and  $\pi/2$  radio-frequency pulses,  $T_2$  is the transverse relaxation time,  $\gamma$  is the gyromagnetic ratio of the nucleus under consideration (the  $^1\text{H}$  nucleus here),  $\Delta$  is the separation of the gradient pulses, and  $\delta$  is the width of the gradient pulses. This equation is often used in a normalized form to remove the effects of transverse relaxation

$$A(G)/A(0) = \exp[-D_s \gamma^2 G^2 \delta^2 (\Delta - \delta/3)] \quad (5)$$

When the value of  $\delta$  is small (i.e., in the narrow pulse limit), the diffusion time is  $\Delta$  and a PGSE experiment is analogous to an incoherent scattering experiment at

scattering vector  $\mathbf{q} = \gamma \delta \mathbf{G}$ . When  $\delta$  is not small, the effective diffusion time is  $\Delta_{\text{eff}} = \Delta - \delta/3$ .

If  $T_2$  is independent of molar mass as is usually found for semidilute binary polymer solutions,<sup>22</sup> this equation can be generalized to apply to a solution of a polydispersed sample with the number distribution  $n(M)$  as

$$\frac{A(k)}{A(0)} = \frac{1}{F} \int_0^\infty \exp[-k D_s(M)] M n(M) dM \quad (6)$$

where

$$A(0) = A_0 \exp(-2\tau/T_2)$$

$$F = \int_0^\infty M n(M) dM$$

and

$$k = \gamma^2 G^2 \delta^2 (\Delta - \delta/3) \quad (7)$$

The analysis of PGSE NMR data on polydisperse polymer samples is very similar to the polydispersity problem in dynamic light scattering. One approach is to follow Koppel's method of cumulants<sup>23</sup> and fit  $\ln [A(k)/A(0)]$  with a power series to obtain the weight-averaged diffusion coefficient, the higher order terms giving the higher order moments of the distribution of diffusion coefficients.<sup>24</sup> The result to second order in  $k$  is

$$\ln [A(k)/A(0)] = -k \langle D \rangle_w + \frac{k^2}{2} (\langle D^2 \rangle_w - \langle D \rangle_w^2) \quad (8)$$

where  $\langle D \rangle_w$  designates the weight-averaged  $D_s$ , given by

$$\langle D \rangle_w = \frac{1}{F} \int_0^\infty D M n(M) dM$$

### 3. Experimental Section

**General Procedures.** The dynamic light scattering experiments were performed using apparatus which has been described previously,<sup>25</sup> except for several modifications which will now be briefly described. The light source is a Spectra Physics 165-08 argon ion laser operated at 488.0 or 514.5 nm. For some measurements a PMS Electro-Optics tunable helium-neon laser (Model No. LSTP-0020) operated at 632.8 nm was used. The lasers were always operated well above threshold and, if necessary, the beam was attenuated with a variable neutral density filter. A microscope stage with  $x$  and  $y$  translation verniers was adapted to fit onto the top of the Malvern Instruments refractive index matching bath so that NMR tubes could be precisely positioned for DLS measurements.<sup>26</sup>

The PGSE NMR experiments were performed on a JEOL FX-60 Fourier transform NMR spectrometer which has been modified for PGSE NMR and NMR imaging experiments as described in refs 27–29. The JEOL software has been supplemented by a program specifically designed to run PGSE experiments. A pulse sequencer designed and built by Eccles<sup>28</sup> allows the TI 980A computer in the spectrometer to control the radio-frequency and magnetic field gradient pulses and the original JEOL preamplifier has been replaced by one with greater gain and signal to noise ratio.<sup>28</sup>

The field gradient pulses are produced by electronically switching the current from a commercial power operational amplifier (Kepco ATE 75-15M) operated in constant current mode as described by Callaghan, Trotter, and Jolley.<sup>27</sup> The Kepco ATE 75-15M power supply has been modified by Xia<sup>29</sup> to reduce the ripple on the output.

A PGSE NMR probe<sup>30</sup> with  $G = 1.215 \text{ T m}^{-1} \text{ A}^{-1}$  was used for these measurements. The high gradients available with this probe made it possible to measure very low diffusion coefficients. The quadrupolar geometry of the gradient coil provides good gradient uniformity along the vertical ( $y$ ) axis, which means that long samples can be used. Homogeneity coils were used to improve the spectral resolution by making fine adjustments to the main

Table I  
Classification of Samples

series	solvent	PVME	$x = C_{PS}/(C_{PS} + C_{PVME})$
D	C <sub>7</sub> H <sub>8</sub>	G-PVME D2	0.001
E6	C <sub>7</sub> D <sub>8</sub>	G-PVME E2	0.056
E11	C <sub>7</sub> D <sub>8</sub>	G-PVME E2	0.114
E25	C <sub>7</sub> D <sub>8</sub>	G-PVME E2	0.246

field. Signal averaging and coherent noise cancellation were always employed, and an exponential filter was applied to the digitized data in the time domain, giving a spectral broadening of approximately 20 Hz.

The calibration of the probe was frequently checked by measuring  $D_s$  for water and checking the results against the precise measurements of Mills.<sup>31</sup>

For routine analysis, linear least-squares fits were used to find the slope and intercept of the plots of  $\ln [A(k)/A(0)]$  against  $k$  (eq 7), the slope being interpreted as  $-D_s$ . In addition to the linear least-squares fitting program which was used for routine data analysis, polynomial fits on a commercial software package (Cricket Graph; Cricket Software) were used.

**DLS and PGSE NMR Experiments on PS-PVME-Toluene.** Both PGSE NMR and DLS experiments were performed on the same samples in this set of experiments. Higher polystyrene concentrations than those previously used in optical tracer DLS experiments were required for the PGSE NMR measurements, so the effect of the additional polystyrene on the results was investigated by varying the proportions of PS and PVME in the solutions.

The concentration of polystyrene as a proportion of the total polymer concentration can be conveniently defined as

$$x = C_{PS}/(C_{PS} + C_{PVME}) \quad (9)$$

where  $C_i$  is the mass/volume concentration of component  $i$ . Samples with four different values of  $x$  were made. One of the samples ( $x = 0.001$ ) contained too little polystyrene for PGSE NMR or DLS measurements of the polystyrene diffusion, but it was still possible to measure the PVME self-diffusion in this sample by PGSE NMR. Lower concentrations of the samples were made by successive dilutions with neat solvent. The characteristics of the four series of samples are summarized in Table I.

The polystyrene used in these experiments was a standard polystyrene with  $M_w = 110\,000\text{ g mol}^{-1}$  and  $M_w/M_n = 1.06$  (Lot 4b), obtained from the Pressure Chemical Co.

The PVME fractions were prepared by batch fractional precipitation of Gantrex M-555 (GAF (Australasia) Auckland, New Zealand), using methods which have been discussed before.<sup>32,33</sup> The fractions were characterized using DLS and sedimentation velocity measurements on dilute solutions of PVME in ethyl acetate.<sup>26</sup> The molar mass of the G-PVME E2 fraction calculated using the Svedberg equation was  $110\,000\text{ g mol}^{-1}$ , and  $M_w/M_n$  was estimated from DLS measurements as 1.3. The value of the diffusion coefficient of fraction G-PVME D2 at infinite dilution was equal within experimental errors to that of G-PVME E2, indicating that the molar mass of the G-PVME D2 fraction was approximately equal to that of the G-PVME E2 fraction.

The deuterated toluene used to make the E series samples was obtained from two sources; CEA, Service des Molécules, Marquées, France (DMM-5, lot 179-780), and the Sigma Chemical Co. (Lot 58C-0099). Each of these solvents had a 99+ % deuteration rating. The undeuterated toluene was a chromatography-grade solvent manufactured by BDH Chemicals, England.

All measurements were made at a temperature of 30 °C.

The compositions of the samples studied in this set of experiments are listed in Table II. Mass/volume concentrations and volume fractions were calculated assuming simple additivity of volumes. The partial specific volume of PVME was taken as  $0.983 \times 10^{-3}\text{ m}^3\text{ kg}^{-1}$ .<sup>34</sup> The partial specific volume of polystyrene in toluene was taken as the value at infinite dilution interpolated to 30 °C using the temperature dependence given by Scholte.<sup>35</sup> The value of  $\bar{v}$  for undeuterated toluene was taken as the reciprocal of the density at 30 °C using the value of  $\rho$  at 25 °C and the temperature coefficient of density given in ref 36.

Table II  
Compositions of Samples,  $T = 30\text{ °C}$

sample name	mass fraction		total polym conc, $C/\text{kg m}^{-3}$	total polym vol fraction, $\phi$
	PS	PVME		
D-1	0.000 30	0.514 63	480.5	0.472
D-2	0.000 25	0.422 65	388.5	0.382
D-3	0.000 18	0.310 41	280.1	0.275
D-4	0.000 12	0.212 30	188.5	0.185
D-5	0.000 08	0.134 91	118.3	0.116
D-6	0.000 05	0.094 48	82.3	0.081
E6-1	0.029 92	0.505 47	525.1	0.514
E6-2	0.025 60	0.432 50	446.3	0.437
E6-3	0.017 99	0.303 83	310.0	0.304
E6-4	0.013 22	0.223 35	226.3	0.222
E6-5	0.008 91	0.150 49	151.5	0.148
E6-6	0.006 70	0.113 21	113.6	0.111
E11-1	0.065 68	0.512 91	570.7	0.557
E11-2	0.053 18	0.415 32	457.6	0.447
E11-3	0.038 87	0.303 56	330.8	0.323
E11-4	0.031 51	0.246 11	266.7	0.260
E11-5	0.017 89	0.139 68	149.8	0.146
E11-6	0.013 36	0.104 34	111.5	0.109
E25-1	0.140 23	0.429 42	564.0	0.546
E25-2	0.092 12	0.282 07	363.6	0.352
E25-3	0.055 86	0.171 05	217.4	0.210
E25-4	0.038 16	0.116 85	147.5	0.143
E25-5	0.025 48	0.078 04	98.1	0.095
E25-6	0.017 94	0.054 95	68.8	0.067

The density of deuterated toluene was calculated approximately by assuming that the volume per molecule remains the same as it is for undeuterated toluene and multiplying  $\rho$  by the ratio of the molar masses (100.15/92.1). This method is suggested in the technical literature provided by a supplier of deuterated solvents.<sup>37</sup>

A limited quantity of fractionated PVME was available, so small samples were necessary. PGSE NMR and DLS experiments were performed on exactly the same samples, so the samples had to be contained in 4-mm-diameter NMR tubes to fit into the high-gradient PGSE probe. Ground-glass sockets were added to the tops of the tubes so that they could be sealed with Teflon stoppers during experiments and then be easily reopened for dilutions. The optical quality of the NMR tubes was adequate for the DLS experiments, but careful alignment was required and stray reflections were carefully avoided.

The sample preparation technique was as follows. Dilute solutions of the fractionated PVME (about  $50\text{ mg g}^{-1}$ ) and polystyrene ( $15\text{ mg g}^{-1}$ ) were made. The PVME solution was filtered into a clean light scattering cell. The solvent was slowly evaporated under an aspirator pump vacuum until the desired PVME concentration and sample volume (about  $100\text{ }\mu\text{L}$ ) was reached. An appropriate quantity of the filtered, dilute polystyrene solution was then added. The solutions were mixed thoroughly over a period of days. The distribution of polystyrene was checked by examining the solution in an unfocused laser beam. The overall concentration was adjusted, if necessary, after addition and mixing of the dilute polystyrene solution by further evaporation of solvent.

When the solutions had mixed completely, they were carefully transferred to the modified NMR tubes for measurements. (The evaporation and mixing steps would have taken far too long if the samples had been contained in NMR tubes from the beginning.) One problem with this method of sample preparation is that some degree of solvent evaporation is inevitable. It was therefore necessary to measure the concentration of the samples again by weighing after the experiments were completed.

Corrections to the refractive indices of the samples due to changes in concentration and wavelength were calculated approximately using equations and data given in refs 34–36.

After each dilution with pure solvent, at least 1 week of equilibration time was allowed. Mixing was assisted by tilting the tube and allowing the solution to slowly flow from one side to the other or gently agitating the more dilute solutions. The uniformity of each sample was then checked by making DLS measurements at several locations along the tube. The sample was allowed to equilibrate until the results were independent of position.

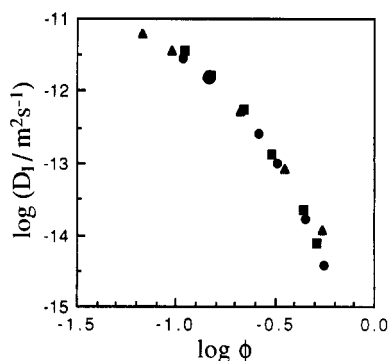


**Figure 1.** Diffusion coefficient obtained from DLS experiments on E6 (■), E11 (●), and E25 (▲) series samples of the PS-PVME-toluene- $d_8$  system. The concentration variable is the total polymer volume fraction,  $\phi$ . The PS and PVME molar masses are both  $110\,000\text{ g mol}^{-1}$  and  $T = 30\text{ }^\circ\text{C}$ .

The DLS experiments were repeated several times over a period of days for each sample. Measurements were made at at least two angles for each sample and three or four angles for some. The correlation functions were well described by second-order cumulant fits at all concentrations, and the results were independent of angle and wavelength, within experimental errors.

At the highest concentrations, long sample times (on the order of 10 ms) were necessary and higher incident power was required producing difficulties due to local heating in the sample. Fluorescence from the samples was observed, indicating that the heating was probably due to strong absorption of the incident light. The local heating produced a thermal lens effect (spatial variation in refractive index due to temperature differences) which enlarged the diameter of the transmitted beam. Correlation functions were also affected by the local heating. Plots of  $\ln S_i$  (where  $S_i$  is the experimental estimate of the electric field autocorrelation function) exhibited a downward curvature due to convection in the sample, and negative values of the quadratic term obtained from cumulant fits  $\mu_2/\langle\Gamma\rangle^2$  were found. The simplest solution to this problem is to reduce the incident power. In some cases, the power had to be reduced so much that measurements became very difficult. Instead of reducing the incident power further, it was more effective to increase the wavelength of the incident light. At longer wavelengths, less fluorescence was observed, presumably because the resonant absorption was no longer occurring. For some of these measurements, it was sufficient to change the wavelength of the Ar ion laser from 488.0 to 514.5 nm, but it was more often necessary to use a He-Ne laser operating at 632.8 nm.

#### 4. Results and Discussion

**Results of DLS Experiments.** Apart from a very weak enhancement of the first channel which was observed in some of the lower concentration data for series E11 and E25, there was no sign of a fast mode for any of the samples studied. In fact, the weak enhancement which was observed could not be distinguished from the distortion caused by photomultiplier afterpulsing which becomes apparent at short sample times and low count rates.

The values of  $D_1$  obtained from quadratic cumulant fits to the DLS data are plotted against the total polymer volume fraction in Figure 1. No systematic variation of  $D_1$  was observed over the range of  $x$  values studied in these experiments. The estimated uncertainty in values of  $D_1$  was generally less than  $\pm 5\%$ , giving error bars of  $\pm 0.02$  on Figure 1. The exception was sample E25-1 (the highest concentration of the E25 series), with an error bar of  $\pm 0.06$ . These uncertainties were estimated from the reproducibility of the measurements. Figure 1 shows that  $D_1$  decreases as the concentration is increased, in keeping with the behavior expected of the interdiffusion mode and the self-diffusion coefficient.

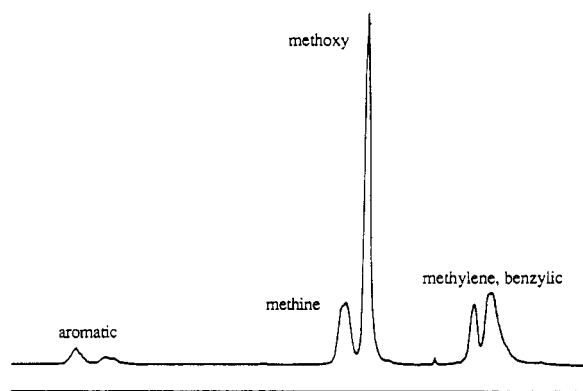


**Figure 2.** High-resolution NMR spectrum of a PS-PVME-toluene- $d_8$  sample with a polymer volume fraction of approximately 0.4 and  $x = 0.11$ , recorded on a JEOL GX270 spectrometer. The aromatic and benzylic protons only occur on the PS and the methoxy and methine protons only occur on the PVME, but methylene protons occur on both PS and PVME.

The values of  $\mu_2/\langle\Gamma\rangle^2$  obtained at higher concentrations were consistently higher than the values obtained at lower concentrations. Samples of the E25 series gave values of  $\mu_2/\langle\Gamma\rangle^2$  which were consistently higher than those obtained for the E6 and E11 series. Typical values of  $\mu_2/\langle\Gamma\rangle^2$  for the E25 samples ranged from 0.25 down to 0.10. For the E6 and E11 samples, the range was from 0.20 down to 0.05. The uncertainty in values of  $\mu_2/\langle\Gamma\rangle^2$  was typically  $\pm 0.05$ . The increase of  $\mu_2/\langle\Gamma\rangle^2$  with increasing polymer concentration seen here is probably due to a broadening of the distribution of diffusion coefficients as the molar mass exponent for  $D_s$  decreases from about  $-0.5$  to  $-2.0$  and possibly further, as discussed by Lodge et al.<sup>6</sup>

**Results of PGSE Experiments.** The relative positions of the peaks in the proton NMR spectra of polystyrene, PVME, and toluene are particularly important to these experiments. A high-resolution spectrum showing the positions of the peaks is given in Figure 2. The form of this spectrum agrees with spectra in the literature.<sup>38-40</sup> The resolution obtained with the PGSE probe was somewhat poorer, but the aromatic region of the spectrum was clearly resolved from the region containing the methine and benzylic peaks. Two spectral windows, covering the aromatic (labeled  $\beta$ ) and nonaromatic (labeled  $\gamma$ ) regions of the spectrum, were used to obtain echo attenuation plots. The  $\beta$  window comprised signals arising only from the polystyrene protons whereas the  $\gamma$  window contained contributions from both polymers, weighted according to the numbers of protons in nonaromatic sites and their respective  $T_2$  attenuation factors. It should be noted that the contributions from the toluene solvent protons overlap with the polystyrene resonances. In the case of the E series samples, where deuterated toluene was used, this contribution was less than 5%. For the D series samples, undeuterated toluene was used and the solvent signal comprised a significant fraction of the total under zero-gradient conditions. In both cases, however, once the field gradient pulses were applied, the vastly different solvent and polymer diffusion coefficients led to extremely rapid solvent signal attenuations. Consequently, the solvent signal influenced only the zero-gradient intercept and not the gradient dependence of the echo attenuation.

The normalized echo attenuation  $A(k)/A(0)$  was measured as a function of  $k$  for three spectral windows in the experiments on the E6, E11, and E25 series samples (see Figure 3). The first window (window  $\alpha$ ) covered all of the peaks and was used by the autophasing routine of our

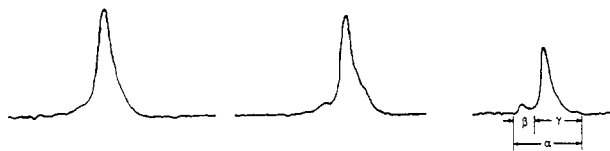


**Figure 3.** Spectra obtained with the PGSE probe at  $\tau = 20$  ms and zero gradient for samples E6-3, E11-3, and E25-2 (left to right). The horizontal scale is the same in all cases, but the vertical scales are arbitrary. Approximate positions of the integration windows ( $\alpha$ ,  $\beta$ ,  $\gamma$ ) are shown. The width of window  $\alpha$  is approximately 36 Hz (6 ppm). The polystyrene aromatic peak becomes better defined as  $x$  is increased.

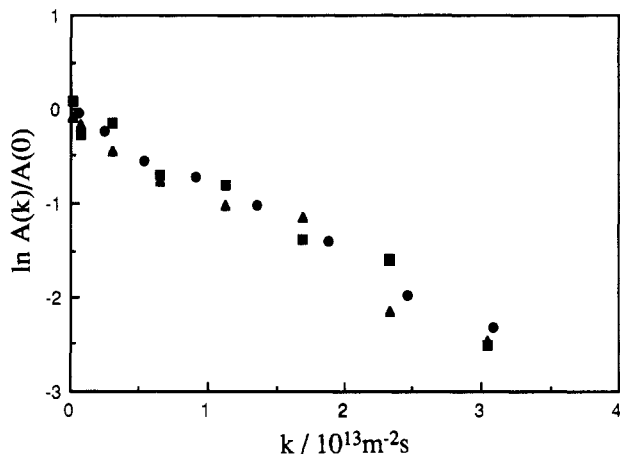


**Figure 4.** Representative echo attenuation plot for window  $\beta$  (sample E6-2). The parameters used in the experiments were as follows:  $\tau = \Delta = 20$  ms,  $G = 10.71$  T m $^{-1}$ ,  $\delta$  varied from 1 to 16 ms ( $\blacksquare$ ,  $\blacktriangle$ );  $\tau = \Delta = 20$  ms,  $G = 11.90$  T m $^{-1}$ ,  $\delta$  varied from 1 to 16 ms ( $\bullet$ ).

PGSE data analysis program to calculate the first-order phase correction. The second spectral window (window  $\beta$ ) covered the peak corresponding to the polystyrene aromatic protons, and the third (window  $\gamma$ ) covered the region containing the PVME methoxy and methine resonances as well as all of the PVME and polystyrene aliphatic (mainly methylene) resonances. Provided that the peaks are sufficiently well resolved and the windows are set appropriately, the echo attenuation plots for window  $\beta$  should directly give the polystyrene self-diffusion coefficient. Plots of  $\ln A(k)/A(0)$  for window  $\beta$  were therefore expected to be linear due to the narrow molar mass distribution of the polystyrene. A representative echo attenuation plot for window  $\beta$  is shown in Figure 4.

The echo attenuation plots for window  $\beta$  were analyzed using linear least-squares fits to  $\ln A(k)/A(0)$ , and a diffusion coefficient, designated as  $D_\beta$ , was calculated from the slope. The echo attenuation plots for window  $\beta$  were often noisy, and they were also sensitive to any small changes in peak position due to interactions between the pulsed field gradient and the field lock circuit. The spectral windows were frequently checked and were adjusted if any small drifts in peak positions had occurred. Within experimental errors, the plots of  $\ln A(k)/A(0)$  for the data from window  $\beta$  were linear, confirming that the self-diffusion coefficient of the polystyrene alone was being measured. Figure 5 shows the concentration dependence of the values of  $D_\beta$  obtained from linear fits to the PGSE NMR echo attenuation plots for window  $\beta$ . The uncertainty in the values of  $D_\beta$  estimated from the reproducibility of measurements was on the order of 10%, giving error bars on the log plot of  $\pm 0.05$ .

Nonlinear plots of  $\ln A(k)/A(0)$  for window  $\gamma$  were expected for both the D and E series samples due to the

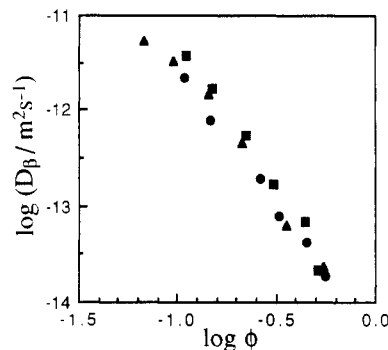


**Figure 5.** Concentration dependence of diffusion coefficients obtained from linear fits to PGSE echo attenuation plots for window  $\beta$ . The results for series E6 ( $\blacksquare$ ), E11 ( $\bullet$ ), and E25 ( $\blacktriangle$ ) are shown. These values are interpreted as the self-diffusion coefficients of the PS in PS-PVME-toluene- $d_8$  solutions at  $T = 30^\circ\text{C}$ .

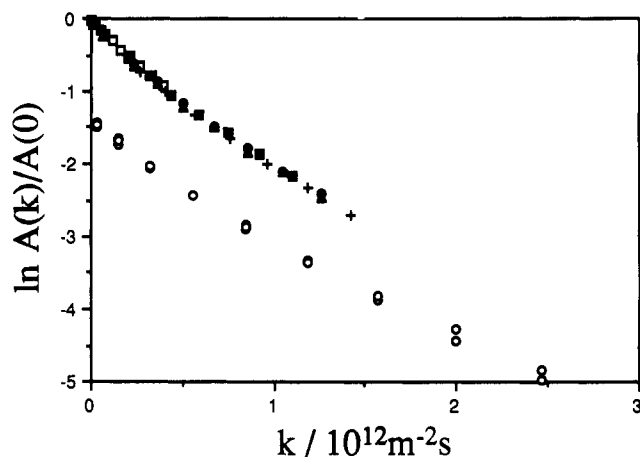


**Figure 6.** Representative echo attenuation plots. (a) For window  $\gamma$  on a D series sample (sample D-5) ( $\circ$ ). The parameters used in the experiments were as follows:  $\tau = \Delta = 15$  ms,  $G = 6.075$  T m $^{-1}$ ,  $\delta$  varied from 1 to 9 ms. The low intercept is due to the rapidly attenuated solvent signal. (b) For window  $\gamma$  on an E series sample (sample E11-6). The parameters used in the experiments were as follows:  $\tau = \Delta = 15$  ms,  $\delta$  varied from 1 to 16 ms;  $G = 2.182$  T m $^{-1}$  ( $\square$ ),  $3.636$  T m $^{-1}$  ( $\blacksquare$ ),  $3.878$  T m $^{-1}$  ( $\bullet$ ,  $\blacktriangle$ ),  $4.121$  T m $^{-1}$  ( $+$ ). These two data sets correspond to roughly equal total polymer concentrations.

polydispersity of the PVME ( $M_w/M_n = 1.3$ ). The non-linearity of  $\ln A(k)/A(0)$  for the E series samples was also expected to contain a small contribution from the PS echo attenuation due to the overlap of PS and PVME peaks (assuming that the PS and PVME have different diffusion coefficients).

Typical echo attenuation plots for window  $\gamma$  obtained from a D series sample and an E series sample are shown in Figure 6. Assuming that  $\ln A(k)/A(0)$  for the D series samples can be adequately described by a second-order polynomial fit, that  $T_2$  is independent of  $M$  at higher concentrations, and that all measurements on a given echo attenuation plot are made with the same value of  $\tau$ , eq 8 can be rearranged to give  $A(k)/A(0)$  as

$$A(k)/A(0) = A_0 \exp\left(-k\langle D \rangle_w + \frac{1}{2}V_D(k\langle D \rangle_w)^2\right) \quad (10)$$

where  $V_D$  is the normalized variance of the distribution of diffusion coefficients, defined as

$$V_D = (\langle D^2 \rangle_w - \langle D \rangle_w^2) / \langle D \rangle_w^2 \quad (11)$$

and  $A_0$  has been introduced to allow for an extremely rapidly attenuated signal from the solvent, giving an intercept differing from 1.0. The form of  $A(k)/A(0)$  for

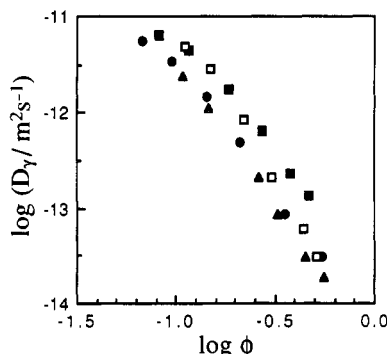


**Figure 7.** Concentration dependence of diffusion coefficients obtained from quadratic or, at the highest concentrations for the E series samples, linear fits to PGSE echo attenuation plots for window  $\gamma$ . The results for series D ( $\blacksquare$ ), E6 ( $\square$ ), E11 ( $\blacktriangle$ ), and E25 ( $\bullet$ ) samples are shown. The diffusion coefficients plotted here can only be definitely identified as the PVME self-diffusion coefficients for the D series samples.

the E series samples was made more complicated by the presence of a contribution from the polystyrene aliphatic protons in window  $\gamma$ . Window  $\gamma$  contains the PS methylene and benzylic resonances as well as the PVME methoxy, methine, and methylene resonances. The polystyrene concentration was small and the PS proton  $T_2$  was shorter than the PVME proton  $T_2$ , so the PS contribution was assumed to be negligible in the data analysis. Therefore, eq 10 was also used to analyze the window  $\gamma$  data for the E series samples. Later, when the diffusion coefficients obtained from window  $\gamma$  are discussed, we will return to this point and conclude that the PS contribution at the experimental values of  $k$  is not negligible, despite the lower concentration and shorter  $T_2$ .

Quadratic fits to  $\ln A(k)/A(0)$  gave an adequate description of the window  $\gamma$  data for the E series samples in most cases except for a few of the high-concentration samples which were better described by linear fits. A self-diffusion coefficient designated as  $D_\gamma$  was obtained from the slope in the case of the linear fits or the initial slope (given by the linear term) in the case of the quadratic fits.

Figure 7 shows the values of  $D_\gamma$  obtained from the initial slopes of quadratic fits to the echo attenuation plots for window  $\gamma$ . The reproducibility of these values was approximately  $\pm 7\%$ , giving error bars on the log plot of  $\pm 0.03$ . The second-order term from the quadratic fits to  $\ln A(k)/A(0)$  gave the variance of the distribution of diffusion coefficients (see eq 11) which tended to take lower values at higher concentrations for the E series samples. The values obtained for the D series samples tended to cluster around 0.12 and remained essentially constant over the entire concentration range.

**Discussion.** Previous work on self-diffusion in polymer solutions has often focused on polystyrene because it is readily available as a well-characterized, monodisperse polymer, but polystyrene solutions suffer from one major limitation—neat polystyrene is a glassy solid at room temperature. At high concentrations, the effective local friction, which is often described in terms of a reduction in free volume, increases due to the proximity of the glass transition and adds complexity to the interpretation of self-diffusion data. It is usually desirable to reduce this effect as much as possible. Many experimentalists have done this by using high molar mass polystyrenes so that the overlap concentration  $C^*$  is low. Concentrations well above  $C^*$  can then be studied while keeping the absolute concentration low and minimizing the free volume effects.

The major polymer component in the solutions studied here is PVME, which has a lower glass transition tem-

perature than polystyrene. The glass transition temperatures of neat PVME and PS measured by Bank et al.<sup>41</sup> were  $-29$  and  $102^\circ\text{C}$ , respectively. This means that PVME is a liquid at room temperature whereas PS is a glassy solid. Even concentrated solutions of PVME are therefore expected to be far above the glass transition at room temperature. This has made it possible to measure self-diffusion at concentrations as high as  $570\text{ kg m}^{-3}$  in this series of experiments.

The overlap concentration  $C^*$  for PVME in toluene was estimated by the following method. The unperturbed  $R_G$  was calculated using the relationship given in ref 34. It was assumed that toluene is a good solvent for PVME, and the expansion factor for the PVME was approximated as 1.3. This value was obtained from data on PS with the same degree of polymerization in toluene. Using the resultant value of  $R_G$ ,  $C^*$  was estimated from  $M/N_A R_G^3$  as  $45\text{ kg m}^{-3}$ , or  $\phi^* = 0.044$ . This value is in agreement with Martin's estimate of  $\phi^*$  for a similar PVME in toluene.<sup>5</sup>

A feature of the light scattering results of this section which is at first surprising is that the cooperative mode was not observed, even when polystyrene comprised almost 25% of the total concentration of polymer in the solution. This can be understood in terms of the theory of Benmouna et al.<sup>14</sup> Their results show that the contribution of the cooperative mode decreases with increasing total polymer concentration at a given value of  $x$  and decreases as  $x$  decreases if the total polymer concentration remains fixed. If  $x$  is less than 0.25 (which is the case in the experiments described here), the contribution of the cooperative mode is less than 15% at the overlap concentration and decreases as the concentration is increased. The ratio of  $D_c$  to  $D_s$  for polystyrene ( $M_w = 110\,000\text{ g mol}^{-1}$ ) in toluene at  $C^*$  is approximately 24.<sup>42,43</sup> Assuming equal mode amplitudes,  $\ln S_i$  for the fast mode would decay to  $-1.4$  in the time taken for the slow mode to decay to  $-0.06$  (this time corresponds approximately to the width of the first channel of our correlator if  $D_{\text{slow}} q^2 \tau_{\text{max}} \approx 3$ ). When these factors are considered, it is quite understandable that the cooperative mode was not observed in these experiments. More favorable conditions for the extraction of both modes from DLS data would exist at  $x$  values of approximately 0.5–0.75. The cooperative mode would have a larger amplitude, but it would decay quickly.

Martin<sup>44</sup> has published results of experiments on the PS-PVME-toluene system which can be directly compared with those presented here. Martin measured the concentration dependence of  $D_s$  for a trace of PS in PVME-toluene solutions at  $26^\circ\text{C}$  for a range of PS molar masses. The polystyrene used in Martin's experiments with the closest molar mass to that used here ( $110\,000\text{ g mol}^{-1}$ ) had  $M_w = 106\,000\text{ g mol}^{-1}$  and  $M_w/M_n = 1.06$ , and the PVME was unfractionated Gantrez M-556 ( $M_w \approx 110\,000\text{ g mol}^{-1}$ ,  $M_w/M_n \approx 2$ ). The results of Martin's experiments taken from his Figure 1 are plotted with the results of this work in Figure 8. Also shown is the value of  $D_0$  for polystyrene ( $110\,000\text{ g mol}^{-1}$ ) in toluene calculated using the relationship between  $D_0$  and  $M$  given by Appelt and Meyerhoff.<sup>45</sup> The Stokes-Einstein equation was used to correct this result for viscosity and temperature differences to  $30^\circ\text{C}$ . The correction required for Martin's results was negligible on the scale of this graph. The results obtained in this work agree well with those of Martin and extend to higher concentrations. The agreement between Martin's results and ours confirms that deuteration of the solvent has a negligible effect on the self-diffusion coefficient of polystyrene, provided that the concentration is expressed in terms of the volume fraction.



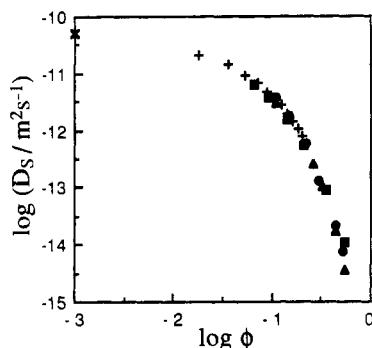


**Figure 8.** Comparison of the self-diffusion coefficients obtained from DLS experiments in this work [E6 (●), E11 (▲), E25 (■)] with those of Martin (+).<sup>44</sup> Also shown, for comparison, is the value of  $D_0$  (×) calculated using the relationship between  $D_0$  and  $M$  given by Appelt and Meyerhoff<sup>45</sup> and corrected for solvent viscosity and temperature differences using the Stokes-Einstein relation to our measurement temperature, 30 °C.

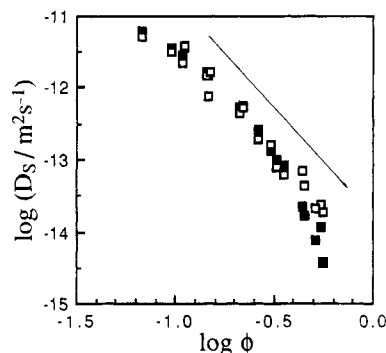


**Figure 9.** Comparison of the self-diffusion coefficients obtained from DLS experiments (■) with those obtained from PGSE experiments on window  $\beta$  (□) at  $T = 30$  °C. The agreement between the two sets of results leads to the conclusion that the diffusion coefficient measured in these DLS experiments is equal to the self-diffusion coefficient of the polystyrene.

Figure 1 shows that the variation of  $D_1$  with  $x$  is very weak, if it exists at all, for the samples studied here. This provides direct experimental confirmation that the product  $A_2 M \chi / v$  appearing in eq 1 is close to zero, giving  $D_1 \approx D_s$  for a considerable range of  $x$  values.

If the arguments presented above are correct and the values of  $D_1$  measured in the experiments reported here are equal to  $D_s$ , they should agree with the values of  $D_\beta$  measured in PGSE NMR experiments on the same samples. Figure 9 gives a comparison of the values of  $D_\beta$  and  $D_1$  obtained from PGSE and DLS measurements. The results of experiments using the two techniques agree within experimental error over most of the concentration range, which suggests that  $D_1$  and  $D_\beta$  are equal and identical to the self-diffusion coefficient of the polystyrene for our samples. A line of slope  $-3$  is also shown in Figure 9 for comparison. This line corresponds to the slope expected for the self-diffusion coefficient of a monodisperse polymer solution in a  $\theta$  solvent or a good solvent above the semidilute-good to semidilute- $\theta$  crossover concentration.

Both the PGSE results and the DLS results are consistent with a  $\phi^{-3}$  concentration dependence between  $\phi = 0.1$  and  $\phi = 0.32$ . A discrepancy between the DLS and PGSE values of  $D_\beta$  is apparent at the highest polymer concentrations. The DLS values appear to fall more rapidly than the PGSE values above volume fractions of approximately 0.4. A possible explanation for the discrepancy is that DLS measures the  $z$ -averaged diffusion coefficient whereas PGSE NMR measures the weight-

averaged diffusion coefficient. Assuming that the PS molecules diffuse independently and using a log-normal distribution to approximate the PS molecular weight distribution, an analysis similar to that performed by Lodge et al.<sup>6</sup> and Callaghan and Pinder<sup>46</sup> gives  $D_w/D_z = 1.03$  for  $\alpha = -0.5$ , 1.0 for  $\alpha = -1$ , and 1.124 for  $\alpha = -2$ . Therefore, it is unlikely that the difference between  $D_z$  and  $D_w$  is totally responsible for the discrepancy at the highest concentrations. Other possible reasons for the discrepancy are distortion of the light scattering data by PS concentration inhomogeneities or particulate contamination which could have sedimented as the polymer concentration was decreased, or a small systematic error in the NMR results which only became significant at the highest concentrations. It should be noted that the diffusion coefficients measured at the highest concentrations are among the lowest ever measured using this technique. The possibility also exists that  $D_1$  measured by DLS is no longer equal to the self-diffusion coefficient of the PS at such high concentrations. If the discrepancy is due to  $\chi$  no longer being close to zero, a positive value of  $\chi$  would be required—this seems unlikely, since it is well-known that PS and PVME are compatible in ternary solution with toluene. More measurements would be required to distinguish between these possibilities.

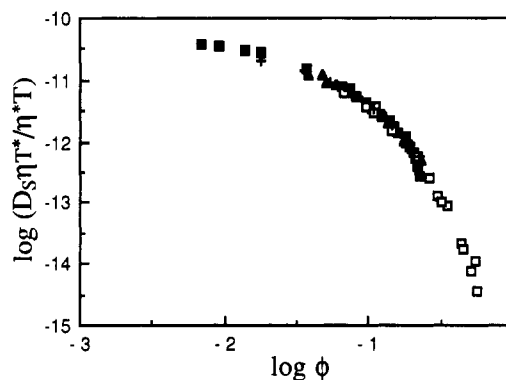
The results of the PGSE NMR measurements on window  $\gamma$  will now be discussed. As was mentioned earlier, the plots of  $\ln A(k)/A(0)$  for data from window  $\gamma$  were nonlinear (see Figure 6). The curvature of the plots for the D series samples was attributed to the polydispersity of the PVME, and quadratic polynomial fits were used to analyze the data. It is possible<sup>46</sup> to estimate the polydispersity of the G-PVME D2 fraction from the quadratic term of the polynomial fits to  $\ln A(k)/A(0)$  using eq 11 if a log-normal molar mass distribution for the PVME is assumed and the value of the exponent in the relationship  $D_0 = aM^{-\alpha}$  is known. Taking  $\alpha = 0.55$  (a typical value for polymer-good solvent systems) and using  $V_D = 0.12$ ,  $M_w/M_n$  is estimated as 1.45. This is consistent with the polydispersity of 1.3 obtained from DLS measurements.<sup>26</sup> This treatment is valid at infinite dilution. The effects of polydispersity at higher concentrations are more complicated. The exponent for the molar mass scaling of the self-diffusion coefficient at semidilute concentrations and in the melt is generally closer to  $-2$ . This result applies to solutions and melts of monodisperse polymers. It has previously been shown by Callaghan and Pinder<sup>22</sup> that a polymer in a polydisperse solution does not have the same diffusion coefficient as it does in a solution of polymers of its own molar mass at the same concentration. This leads to a narrower distribution of diffusion coefficients than would be expected on the basis of the naive approach of substituting the semidilute molar mass scaling exponent for  $\alpha$  in the treatment described above.

Figure 7 shows the concentration dependence of the diffusion coefficients obtained from the window  $\gamma$  data. As was mentioned earlier,  $D_\gamma$  was assumed to be equal to the PVME diffusion coefficient in these measurements. The values of  $D_\gamma$  for samples with very low PS concentrations (the D series) fall on a smooth curve which tends to power law behavior at higher concentrations. The reptation model suggests that the concentration scaling exponent should be  $-1.75$  for a polymer in a good solvent and  $-3$  for a polymer in a  $\theta$  solvent. When the blob model is applied to self-diffusion, it predicts that the concentration scaling exponent of  $D_s$  should gradually change from  $-1.75$  to  $-3$  as the concentration increases.<sup>47</sup> The behavior of  $D_s$  for PVME in the D samples shown in Figure

7 is consistent with the description provided by the blob model. The absence of an extended  $C^{-1.75}$  scaling region is explained by the fact that the semidilute-good to semidilute- $\theta$  crossover occurs quite close to  $C^*$  for low molar masses. The observation of an extended  $C^{-3}$  scaling region for polystyrene in a good solvent at high concentrations is made difficult by the onset of an increase in the local friction related to a reduction in free volume, but this effect is obviously comparatively weak in PVME solutions.

The  $D_\gamma$  values for the E series samples shown in Figure 7 display unexpected behavior. Most of the points fall below the  $D_\gamma$  values obtained for the D series samples. At high concentrations, the  $D_\gamma$  values for the E6 samples are in agreement with the E11 and E25 data and, at low concentrations, they agree better with the D series values. At first sight, it might seem that the presence of a significant polystyrene component in the E series samples changed the diffusion coefficient of the PVME. In fact this is most unlikely since the polystyrene comprised at most 25% of the total polymer. Any direct interaction between the polymers would have been more likely to influence the polystyrene self-diffusion coefficients, something that is not observed in this work. The best explanation arises from the fact that the  $\gamma$  window contained contributions from both the polystyrene and PVME protons. Careful analysis of respective  $T_2$  values shows that the polystyrene contribution is less than would be expected on the basis of relative nonaromatic proton numbers alone. Despite this reduction, however, their remaining influence is insidious. Because the PVME diffusion coefficients are systematically higher than those of polystyrene, the PVME signal is attenuated more rapidly in the echo attenuation plot, leaving a slowly decaying contribution from the PS at higher values of  $k$ . This produces a bias in the cumulant fit to  $\ln A(k)/A(0)$  used to derive the initial slope. The large values of  $k$  used in this work, combined with the polydispersity of the PVME, produced a systematic bias of the results of the fits to the echo attenuation plots toward the slower PS self-diffusion coefficient rather than the average PVME self-diffusion coefficient which was expected to dominate the initial slope. A comparison of Figures 5 and 7 shows the similarity of the  $D_\gamma$  and the  $D_\beta$  values. This explains why the results from window  $\beta$  gave the PS self-diffusion coefficient despite the poor spectral resolution of the PS aromatic resonance. It also explains why the  $D_\gamma$  values for the E6 series samples tended toward the results obtained for the D series samples as the concentration decreased. Another feature of the results which is consistent with this explanation is the decrease of  $V_D$  for the window  $\gamma$  echo attenuation plots at higher polymer concentrations. Linear plots of  $\ln A(k)/A(0)$  were obtained at the highest polymer concentrations of the E series samples but not for the D series samples.

These ideas were tested by reanalyzing the data for window  $\alpha$  for sample E6-3. The large  $k$  portion of the echo attenuation plot was linear, suggesting that it was due to the PS. Extrapolation of this portion back to the  $k = 0$  intercept gave a relative amplitude for this mode of 0.41. This is greater than expected on the basis of the number densities of the protons contributing to the PVME and PS resonances but could be in error because the PVME echo attenuation contained a slowly decaying component due to polydispersity. The exponential decay with an amplitude of 0.41 and a diffusion coefficient given by the long time, linear part of the echo attenuation plot was subtracted from  $A(k)/A(0)$ , and the resultant echo attenuation plot was fitted with a quadratic, giving a PVME



**Figure 10.** Comparison of PS self-diffusion coefficients in different systems. Unfilled squares represent our DLS results, pluses represent Martin's results, and the filled symbols represent PS self-diffusion coefficients measured by PGSE NMR in PS-benzene- $d_6$  ( $\blacktriangle$ ) and PS- $\text{CCl}_4$  ( $\blacksquare$ ) solutions.<sup>48</sup> In all cases, the PS molar mass was 110 000 g mol<sup>-1</sup>. The PS-benzene- $d_6$  and PS- $\text{CCl}_4$  results have been corrected to  $T = 30^\circ\text{C}$  to account for temperature and solvent viscosity differences.

diffusion coefficient in agreement with the D series curve at the appropriate concentration. A closer examination of the shape of other echo attenuation plots for the E series samples confirmed the existence of a rapidly decaying component and a linear decay at large  $k$  values consistent with this explanation.

A more correct analysis of the data would involve fitting echo attenuation plots for windows  $\alpha$  or  $\gamma$  with eq 14. However, the large number of parameters fitted would require more precise data over a larger range of  $k$  values than was investigated here. Attempts to fit the data with functional forms similar to eq 14 were not successful due to the nonconvergence of the nonlinear curve-fitting algorithm.

Figure 10 gives a comparison of the concentration dependence of the PS self-diffusion coefficient obtained here with that obtained for other systems. It is a remarkable feature of these results that the PS self-diffusion coefficient, corrected for solvent viscosity and temperature, is the same in PVME + toluene as it is in benzene and carbon tetrachloride.<sup>48</sup> (The results for the PS-toluene- $d_8$  system given in ref 42 also agree but cover a smaller concentration range. For the sake of clarity, they are not shown in Figure 10.) This implies that the chemical difference between PS and PVME makes little difference to the self-diffusion of PS, confirming that  $\chi$  is indeed small for solutions of PS and PVME in toluene and that PS and PVME do not form long-lived aggregates in PS-PVME-toluene solutions.

If there is any difference between the behavior of PS solutions and the PS-PVME solutions shown in Figure 10, it is that the PS- $\text{CCl}_4$  data begin to fall rapidly due to effective local viscosity effects (proximity to the glass transition) at high concentrations, whereas the PS-PVME-toluene data are less dramatically affected.

## 5. Conclusions

We have presented the results of dynamic light scattering and pulsed gradient spin-echo NMR measurements on ternary solutions of poly(vinyl methyl ether) (PVME) and polystyrene (PS) in toluene and toluene- $d_8$ . The molar masses of the PVME and PS were 110 000 g mol<sup>-1</sup>, the ratio  $x$  of PS concentration to the total polymer concentration was varied between 0.001 and 0.246, and the total polymer concentration  $C$  was varied between approximately 70 and 500 kg m<sup>-3</sup> for each value of  $x$ .



By performing DLS and PGSE NMR measurements on the same samples, we have directly confirmed, without the need for chemical labeling, that DLS experiments on PS-PVME-toluene solutions give the self-diffusion coefficient of the polystyrene for total polymer fractions up to 0.4. Above  $\phi = 0.4$ , the DLS results are lower than the PGSE NMR results.

The PGSE and DLS results for the PS self-diffusion coefficients showed that  $D_s$  was independent of  $x$  up to  $x = 0.246$  and over a wide range of  $C$ . The observation that the slow-mode diffusion coefficient  $D_l$  obtained from DLS experiments on our ternary solutions is equal to  $D_s$  regardless of the value of  $x$  is consistent with the prediction of the theory of Benmouna et al.,<sup>14</sup> when the value of  $\chi$  (the PS-PVME interaction parameter) is taken as zero.

Excellent agreement between PS self-diffusion coefficients in PS-PVME-toluene- $d_8$  solutions and those obtained previously for binary PS-solvent systems was found after temperature and solvent viscosity corrections were made. This result shows that the chemical difference between PS and PVME has an insignificant effect on the diffusion of the PS and is consistent with the fact that  $\chi$  is small and negative for the PS-PVME pair. The assumption that PS self-diffusion in binary PS-solvent systems is equivalent to that of PS in PS-PVME-toluene solutions has been discussed by Lodge et al.<sup>12</sup> They used the equivalence of the radius of gyration of PS in PS-PVME-toluene solutions with that of PS in binary PS-solvent solutions as supporting evidence for the assumption. The results given here provide more direct support for their argument.

We have also presented the results of our PGSE NMR measurements of  $D_s$  as a function of concentration for PVME in PVME-toluene solutions. The results of these measurements, the first to be obtained for PVME, give clear evidence of  $C^{-3}$  scaling for  $D_s$ , consistent with the reptation model results for solutions above the semidilute-good solvent to semidilute- $\Theta$  solvent crossover.

**Acknowledgment.** We are indebted to Associate Prof. K. W. Jolley for assistance with the measurement of high-resolution spectra and relaxation times on the JEOL GX270 NMR spectrometer.

## References and Notes

- (1) Lodge, T. P. *Macromolecules* **1983**, *16*, 1393.
- (2) Cotts, D. B. *J. Polym. Sci., Polym. Phys. Ed.* **1983**, *21*, 1381.
- (3) Hanley, B.; Balloge, S.; Tirrell, M. *Chem. Eng. Commun.* **1983**, *24*, 93.
- (4) Hanley, B.; Tirrell, M.; Lodge, T. *Polym. Bull. (Berlin)* **1983**, *14*, 137.
- (5) Martin, J. E. *Macromolecules* **1984**, *17*, 1279.
- (6) Lodge, T. P.; Wheeler, L. M.; Hanley, B.; Tirrell, M. *Polym. Bull. (Berlin)* **1986**, *15*, 35.
- (7) Lodge, T. P.; Wheeler, L. M. *Macromolecules* **1986**, *19*, 2983.
- (8) Wheeler, L. M.; Lodge, T. P.; Hanley, B.; Tirrell, M. *Macromolecules* **1987**, *20*, 1120.
- (9) Lodge, T. P.; Markland, P. *Polymer* **1987**, *28*, 1377.
- (10) Chang, T.; Han, C. C.; Wheeler, L. M.; Lodge, T. P. *Macromolecules* **1988**, *21*, 1870.
- (11) Wheeler, L. M.; Lodge, T. P. *Macromolecules* **1989**, *22*, 3399.
- (12) Lodge, T. P.; Markland, P.; Wheeler, L. M. *Macromolecules* **1989**, *22*, 3409.
- (13) Daivis, P. J.; Pinder, D. N. In preparation.
- (14) Benmouna, M.; Benoit, H.; Duval, M.; Akcasu, Z. *Macromolecules* **1987**, *20*, 1107.
- (15) Foley, G.; Cohen, C. *Macromolecules* **1987**, *20*, 1891.
- (16) Borsali, R.; Duval, M.; Benoit, H.; Benmouna, M. *Macromolecules* **1987**, *20*, 1112.
- (17) Borsali, R.; Duval, M.; Benmouna, M. *Macromolecules* **1989**, *22*, 816.
- (18) Klotz, S.; Cantow, H.-J.; Kögler, G. *Polym. Bull. (Berlin)* **1985**, *14*, 143.
- (19) Klotz, S.; Schuster, R. H.; Cantow, H.-J. *Makromol. Chem.* **1986**, *187*, 1491.
- (20) Callaghan, P. T. *Aust. J. Phys.* **1984**, *37*, 359.
- (21) Stejskal, E. O.; Tanner, J. E. *J. Chem. Phys.* **1965**, *42*, 288.
- (22) Callaghan, P. T.; Pinder, D. N. *Macromolecules* **1985**, *18*, 373.
- (23) Koppel, D. E. *J. Chem. Phys.* **1972**, *57*, 4814.
- (24) Callaghan, P. T.; Pinder, D. N. *Macromolecules* **1983**, *16*, 968.
- (25) O'Driscoll, R. C.; Pinder, D. N. *J. Phys. E: Sci. Instrum.* **1980**, *13*, 192.
- (26) Daivis, P. J. Ph.D. Thesis, Massey University, Palmerston North, New Zealand, 1989.
- (27) Callaghan, P. T.; Trotter, C. M.; Jolley, K. W. *J. Magn. Reson.* **1980**, *37*, 247.
- (28) Eccles, C. D. Ph.D. Thesis, Massey University, Palmerston North, New Zealand, 1987.
- (29) Xia, Y. M. Sc. Thesis, Massey University, Palmerston North, New Zealand, 1988.
- (30) Callaghan, P. T. Unpublished.
- (31) Mills, R. *J. Phys. Chem.* **1973**, *77*, 685.
- (32) Manson, J. A.; Arquette, G. J. *Makromol. Chem.* **1960**, *37*, 187.
- (33) Bauer, B. J.; Hanley, B.; Muroga, Y. *Polym. Commun.* **1989**, *30*, 19.
- (34) *Polymer Handbook*; Brandrup, J.; Immergut, E. H., Eds.; John Wiley and Sons: New York, 1975.
- (35) Scholte, Th. G. *J. Polym. Sci.* **1970**, *A2*, 841.
- (36) Johnson, B. L.; Smith, J. *Refractive Indices and Densities of Some Common Polymer Solvents*. In *Light Scattering from Polymer Solutions*; Huglin, M. B., Ed.; Academic Press: London, 1972.
- (37) BDH Chemicals, England.
- (38) Caravatti, P.; Neuenschwander, P.; Ernst, R. R. *Macromolecules* **1985**, *18*, 119.
- (39) Crowther, M. W.; Cabasso, I.; Levy, G. C. *Macromolecules* **1988**, *21*, 2924.
- (40) Mirau, P. A.; Tanaka, H.; Bovey, F. A. *Macromolecules* **1988**, *21*, 2929.
- (41) Bank, M.; Leffingwell, J.; Thies, C. *Macromolecules* **1971**, *4*, 43.
- (42) Callaghan, P. T.; Pinder, D. N. *Polym. Bull.* **1981**, *5*, 305.
- (43) Roots, J.; Nyström, B.; Sundelöf, L.-O.; Porsch, B. *Polymer* **1979**, *20*, 337.
- (44) Martin, J. E. *Macromolecules* **1986**, *19*, 922.
- (45) Appelt, B.; Meyerhoff, G. *Macromolecules* **1980**, *13*, 657.
- (46) Callaghan, P. T.; Pinder, D. N. *Macromolecules* **1983**, *16*, 968. Note that this paper contains an error. The correct expression for  $V_D$  in the case of a log-normal distribution is  $V_D = (M_w/M_n)^{\alpha^2} - 1$ .
- (47) Daivis, P. J.; Pinder, D. N. *Macromolecules* **1990**, *23*, 5176.
- (48) Callaghan, P. T.; Pinder, D. N. *Macromolecules* **1984**, *17*, 431.

**Registry No.** PS (homopolymer), 9003-53-6; Gantrez M-555, 9003-09-2.